INFLUENCIA DE LA GEOMETRÍA EN LOS MÁXIMOS DE LAS TENSIONES EN AJUSTES POR INTERFERENCIA CON AGUJEROS RANURADOS

Miguel Ángel Lorenzo-Fernández, Carmen Blanco-Herrera, Pablo Moreno-Pedráz y Juan Carlos Pérez-Cerdán

Universidad de Salamanca. Avda. Fernando Ballesteros, 2 – 37700 Béjar (Salamanca). Tfno: +34 923 408080. mlorenzo@usal.es

Received: 11/feb/2015 - Accepted: 25/feb/2015 - DOI: http://dx.doi.org/10.6036/7560

INFLUENCE OF GEOMETRY ON THE STRESS PEAKS IN INTERFERENCE FITS WITH GROOVED HUB

ABSTRACT:
Elastic stress distributions in interference fits match the values predicted by pressure cylinders theory only if the two joined parts have the same length. In fact, a heavy stress concentration in the radial component appears at the edges of the contact zone being more intense in the case of the hub. Many methods have been proposed for relieving the stress peaks. In order to investigate how the stress concentrations are reduced, in this paper, different stress analysis in interference fits with grooved hubs were carried out using the finite element method.

Keywords: fit, interference, notch, stress concentrations, finite element analysis

RESUMEN:
Las distribuciones de tensiones elásticas en ajustes por interferencia se ajustan a los valores dados por la teoría de cilindros a presión sólo si los dos piezas unidas tienen la misma longitud. De hecho, una fuerte concentración en la componente radial de la tensión aparece en los bordes de la zona de contacto siendo más intensa dicha concentración en el caso del agujero.
Muchos métodos han sido propuestos para relajar los picos de la tensión. Con el fin de investigar cómo se produce la concentración tensional, en este artículo se llevan a cabo diversos análisis de las tensiones en ajustes por interferencia con agujeros ranurados por medio del método de los elementos finitos.

Palabras clave: ajuste, interferencia, concentración tensional, análisis por elementos finitos

1.- INTRODUCTION

Press or shrink fitting joints are widely used in mechanical engineering to transmit a torque through the joint of two parts because of their high efficiency and easy implementation. Therefore, an adequate understanding of the stress and strains generated by this procedure in fitted parts is a key issue for a right design of these mechanical components. An example of this sort of assemblies is the shaft-hub fitting coupled with pulley and gear system.

The complete characterization of the mechanical behaviour of the assembled elements was already studied both theoretically [1] and experimentally [2] years ago. The main difficulty in such analysis is the dependence of stress states on multiple variables which make complicated the use of theoretical models providing complex analytical solutions [3]. To overcome this shortcoming, the finite element method (FEM) has been widely used for studying different issues of the contact stresses and deformations between cylindrical shafts and hubs [4-8]. Results shows that the stress values at the middle of the contact surface match the ones given by Lamé equations. However, undesirable stress concentrations take place at the hub edges [4,5,9,10]. Many solutions have been proposed to relieve the stress peaks considering a variable radial interference [11] or, more commonly, a hub geometry that significantly modifies the stresses field [9,12,13].

The comparison of the experimental results with the modeling results remains a difficult task because the interface shaft-hub is not accessible to place strain gauges. However, some techniques have been used to avoid this inconvenience.

Publicaciones DYNA SL -- c) Mazarredo nº69 - 4º -- 48009-BILBAO (SPAIN)
Tel +34 944 237 566 – www.revistadyna.com - email: dyna@revistadyna.com

Photoelastic experimental analysis of stress in interference fits [14] are being carried out although, as it is well known, these procedures are applicable only to birefringent materials. To solve this shortcoming, in the recent times new experimental methods were developed based on the reflexion of ultrasonic waves for obtaining the contact pressure distribution in diverse types of fits [15], but, because of measurement uncertainties, the accurately determination of the edge effects is not possible. The technique of neutron diffraction has also been used to measure the stresses generated during a shrink fit subjected to torsional stress [16].

The aim of this work is to analyse the effect of milling a groove on the hub extremities [17-19] on the stress concentrations at the contact surface in interference fits. It must be remarked that at the interface close to a hub edge, where the highest stresses occurs, the contacting surfaces may undergo fretting, which leads to damage and wear, reducing dramatically the life of mechanical parts [20-21]. The present study is carried out by means of numerical simulations with a commercial FEM code. The usefulness of such a hub modification as a procedure to modify the stress state on demand is also assessed. This achievement was obtained analysing the stress concentration factors as a function of parameters defining the geometry of the fit.

2.- THEORETICAL BACKGROUND

Radial and hoop stresses which are present in both cylinders can be deduced from the thick walled pressure cylinders theory based on the Lamé equations [22]. According to these expressions, both stresses in the internal cylinder (or shaft), which is assumed to be solid, are equal to the contact pressure but with opposite sign:

$$\sigma_{r,i} = \sigma_{\theta,i} = -p \qquad (1)$$

whereas the same magnitudes vary with the radial coordinate, r, in the external cylinder (or hub) according to the following equations:

$$\sigma_{r,o}(r) = \frac{pR^2}{r_o^2 - R^2}\left(1 - \frac{r_o^2}{r^2}\right) \qquad (2)$$

$$\sigma_{\theta,o}(r) = \frac{pR^2}{r_o^2 - R^2}\left(1 + \frac{r_o^2}{r^2}\right) \qquad (3)$$

where p is the contact pressure, R is the transition radius and r_o is the hub external radius, i.e., $r_o=R + t$, being t the hub thickness (see Fig. 1b). From the previous formulae it is easy to obtain the von Mises equivalent stress for each component:

$$\sigma_{vM,i} = p \qquad (4)$$

$$\sigma_{vM,o}(r) = \frac{pR^2}{r_o^2 - R^2}\sqrt{1 + 3\left(\frac{r_o^2}{r^2}\right)^2} \qquad (5)$$

These equations are valid if two conditions are fulfilled: the plane strain assumption can be applied and the length of both cylinders must be the same. On the other hand, the value of the radial interference, δ, needed to achieve a given contact pressure p in an interference fit considering both parts made of the same material, can be obtained with the following expression:

$$\delta = \frac{pR}{E}\left(\frac{2r_o^2}{r_o^2 - R^2}\right) \qquad (6)$$

Publicaciones DYNA SL -- c) Mazarredo nº69 - 4º -- 48009-BILBAO (SPAIN)
Tel +34 944 237 566 – www.revistadyna.com - email: dyna@revistadyna.com

3.- NUMERICAL MODELLING

The assumption of axisymmetric geometry can be applied in the simulations. Therefore, the 3D problem (Fig. 1a) is reduced to 2D with a remarkable saving of computing time. Cylindrical coordinates (r, θ, z) are used with the origin placed at the centre of the inner cylinder (Fig. 1b). The plane of symmetry $z = 0$ contains the central cross section of both cylinders and the coordinate $r = R$ represents the contact surface of the cylinders (see Fig. 1b).

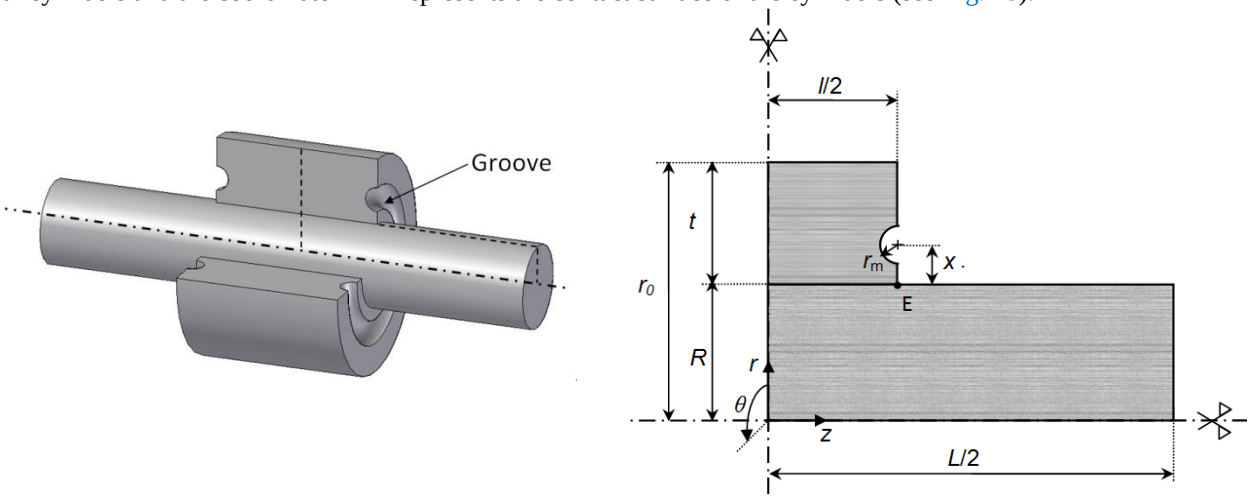

(a) (b)

Fig. 1. (a) General view and (b) Geometrical parameters for the shaft-hub fit and the milled notch.

MSC. Marc FEM code was used to perform the finite element simulation. The meshing of each component was carried out separately. A simple uniformly distributed mesh of 4-nodes quadrilateral elements was considered as Fig. 2 shows taking in mind that the same element size in both components adjusted must be considered at the interface ($r = R$). Thus, at each point located at the interface two superposed nodes are placed. Diverse meshes were tested until the required convergence in results was achieved needing a finer mesh around the notch. For the optimal mesh it has been found a 0.625x0.625 mm element size at contact for both components.

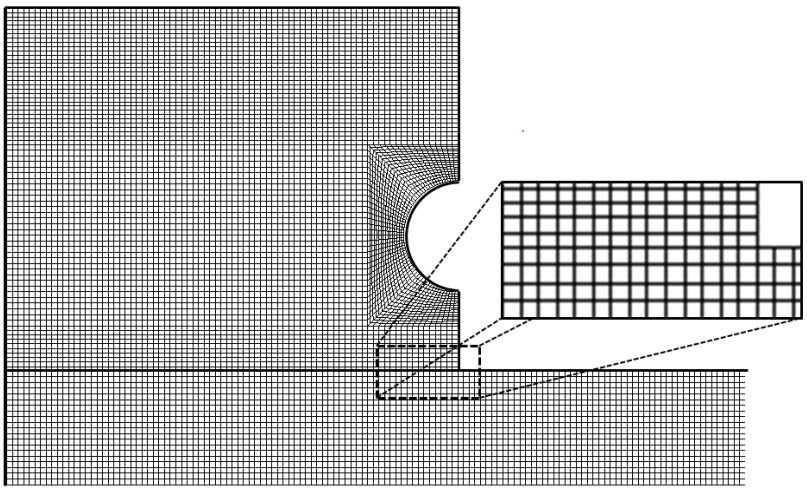

Fig. 2. Sample of the meshing of one of the interference fit cases analysed.

The components of an interference fit are assumed to work within the elastic regime. So far, only two parameters are needed to characterize the mechanical behaviour of the material in the FEM simulation: the Young modulus (E) and the Poisson ratio (v). A standard steel used in mechanical engineering (E = 210 GPa and v = 0.3) was considered. Contact is modelled frictionless (according to [17] no significant changes were found when friction is taken into account). The

Publicaciones DYNA SL -- c) Mazarredo nº69 - 4º -- 48009-BILBAO (SPAIN)
Tel +34 944 237 566 – www.revistadyna.com - email: dyna@revistadyna.com

simulations of the surface to surface contact fit requires considering non linear analysis. The simulations of the surface to surface fit requires considering non linear analysis by contact interface conditions [23]. In our case, that has been done using the specific module included in MARC for simulating situations where bodies with overlaps or gaps in the geometry are required to fit together.

At the interface, i.e., at $r = R$, Eq. (2), (3), and (5) predict a constant stress distributions. However, the assumption of a uniform distribution of pressure p is not appropriate when the components of the interference fit have different length, since the discontinuities in the contact zone lead to a generation of local stress concentrations. In fact, the radial component, of compressive nature in both cylinders, presents important stress concentrations at the edges of the interface of both parts, being more pronounced in the hub [5,24]. Furthermore, hoop stress is tensile in hub. So, it seems reasonable to focus the analysis exclusively on the outer element as it will be done hereafter.

Despite the radial component of stress tensor exhibits the highest stress concentration, the highest absolute values were reached for the hoop stress over the contact zone but with lower stress concentrations. According to these results, stress concentration factors (SCFs) have been introduced, in a similar way as in [17,24]:

$$K_j = \frac{\sigma_{j,FEM\,\max}}{\sigma_{j,th}} \qquad j \equiv r,\ \theta,\ vM \qquad (7)$$

where $\sigma_{j,FEM}$ is the value of stress obtained by means of FEM, being $\sigma_{j,FEM\max}$ the maximum value of the stress distribution, and $\sigma_{j,th}$ is the corresponding value derived from Eq. (2), (3), and (5), both for $r = R$. The subindexes $j \equiv r$, θ, vM refer to radial, hoop and von Mises stresses, respectively.

The groove geometry can be described by two parameters: the notch radius, r_m, and the distance from the notch center to the contact zone, x (in Fig. 1(b) the distance from the notch centre to point E). We have defined two dimensionless parameters $\lambda = r_m/x$ (in a similar problem, analysing an indenter with a notch comprising a half plane [25], the reciprocal parameter of λ, $\eta = 1/2\ \lambda$, is used) and $\xi = r_m/(t/2)$, where $t/2$ is the half-thickness of the hub.

4.- STRESS CONCENTRATION FACTORS

4.1.- INFLUENCE OF THE INTERFERENCE, δ

According to the ISO nomenclature for fits and tolerances, the fit chosen is 200 H7/s6, medium-drive fit type. This fit is recommended for those cases where assembled steel elements need to turn together. Within the limits stated for this type of fit, three different radial interferences were used: δ_{max}= 75.50 μm, δ_{med}= 56.75 μm, δ_{min}= 38.00 μm.

In this simulation, the base fit geometry is given by the length ratio L/l =4 between the shaft length (L) and hub length (l), and hub thickness t = 40 mm. Two cases are considered in terms of dimensionless parameters λ and ξ; $(\lambda, \xi)_1$= (0.600, 0.375) and $(\lambda, \xi)_2$= (0.530, 0.500).

A linear relationship between stress state and radial interference, δ, exists even when a notch has been milled on the hub. So, the relationship between numerically and theoretically obtained stresses is independent on δ value. The SCFs at the interface, calculated according to Eq. (7), raise an identical value for the three interferences values considered as Table 1 shows (this result coincides with reference [24] for an unnotched hub, where K_{vM} is studied only).

Publicaciones DYNA SL -- c) Mazarredo nº69 - 4º -- 48009-BILBAO (SPAIN)
Tel +34 944 237 566 – www.revistadyna.com - email: dyna@revistadyna.com

	K_r	K_θ	K_{vM}
$(\lambda, \xi)_1$	1.16	1.17	1.08
$(\lambda, \xi)_2$	1.03	1.15	1.09

Table 1. SCFs calculated according to Eq. (7) in a notched hub at interface contact cylinders for radial interference values δ_{max}= 75.50 μm, δ_{med}= 56.75 μm, δ_{min}= 38.00 μm.

4.2.- INFLUENCE OF THE *LENGTH RATIO L/l*

The dependence of the K_θ and K_r factors of the hub on the length ratio L/l was also studied for seven different cases, namely, L/l = 8.0, 4.0, 2.0, 1.5, 1.2, 1.1 and 1.0, being δ_{max} = 75.50 μm, and the other parameters equal to those used in previous section.

Slightly variations in the values of stress factors are observed in Fig. 3, within the range $1.01 < K_j < 1.17$ for all cases. For values of $L/l < 2$, the K_j factors decrease and get closer to 1, which corresponds with pressure cylinders theory when the length ratio condition $L/l = 1$ is satisfied. Contrary, if $L/l \geq 2$, the shaft can be consider as an infinitely long element and the constriction due to the edge effect does not varies and thereby the same SCF is obtained (Fig. 3).

Values of the radial stress concentrations factors K_r depend significantly on (λ, ξ) case, but no K_θ and K_{vM}. Notice that for $(\lambda, \xi)_2$ case, the values of K_r are close to 1, and always lower than 1.03 for any length ratio L/l.

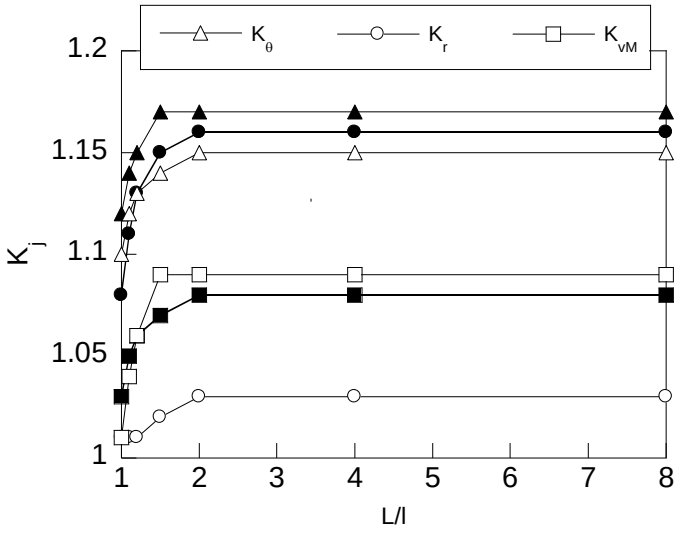

Fig. 3. Stress concentration factors calculated at the interface as a function of L/l. Open symbols corresponding to $(\lambda, \xi)_1$ and filled symbols to $(\lambda, \xi)_2$

4.3.- INFLUENCE OF THE RADII RATIO, R/r_0

The variation of the SCFs as a function of the hub radial ratios R/r_0 at $r = R$ is represented in Fig. 4. Values of this ratio from 0.5 to 0.7 are optimal [26]. The other parameters needed for simulation take the same values as in previous section with L/l = 4. It can be observed that K_{vM} factor is nearly independent on the radii ratio, while K_r increases as ratio R/r_0

Publicaciones DYNA SL -- c) Mazarredo nº69 - 4º -- 48009-BILBAO (SPAIN)
Tel +34 944 237 566 – www.revistadyna.com - email: dyna@revistadyna.com

decreases. K_θ has the opposite behaviour. Thus, the K_j factor which reaches the maximum values is K_θ for the lowest value of R/r_o. For un-grooved hubs, variation of K_{vM} with R/r_0 is also studied in [24]. However, a direct comparison cannot be made since reference [24] calculation analyse shaft-hub configurations which are not considered here.

The more remarkable differences observed between the analysed (λ, ξ) cases occur for the radial stress concentration factor K_r. Unlike K_r, K_θ and K_{vM} SCFs calculated for $(\lambda, \xi)_1$ and $(\lambda, \xi)_2$ converge for higher values of the radii ratio R_0/r.

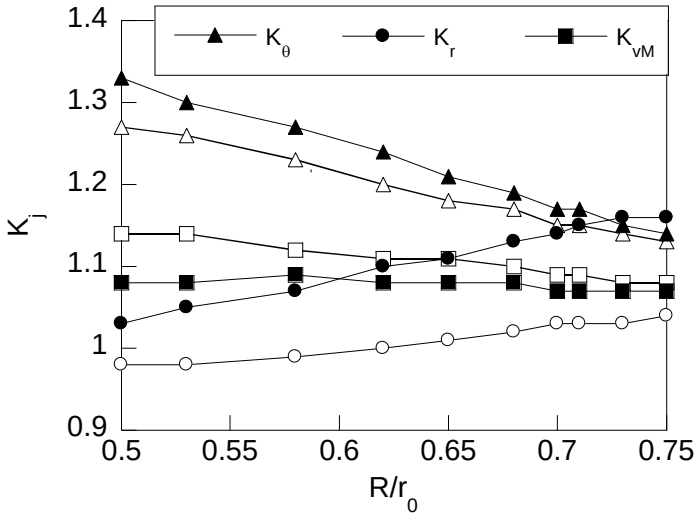

Fig. 4. Stress concentration factors K_j calculated at the interface as a function of radii ratio, R/r_0. Filled symbols corresponding to $(\lambda, \xi)_1$ and open symbols to $(\lambda, \xi)_2$.

4.4.- INFLUENCE OF THE RELATIVE SIZE OF THE NOTCHED HUB, $2r_m/l$

The size (r_m) and the distance of the notch from interface (x) modify the stress concentration at surface. In order to visualize this effect, the distributions of the radial stress obtained from numerical simulation are shown in Fig. 5 for the following cases: (i) unnotched hub (Fig. 5a), a hub with (ii) low notch radius placed close to interface (Fig. 5b), (iii) a high notch radius placed close to interface (Fig. 5c) and, finally, (iv) a high notch radius placed far away from interface (Fig. 5d). From these distributions is revealed the different effect of the notch geometry on the stress concentration at interface. This way, the stress concentration located at the edge of the interface significantly decreases when the notch is placed close to interface (Fig. 5b and Fig. 5c), whereas is slightly affected if the distance to interference is high enough (Fig. 5d), even for the same notch radius.

Publicaciones DYNA SL -- c) Mazarredo nº69 - 4º -- 48009-BILBAO (SPAIN)
Tel +34 944 237 566 – www.revistadyna.com - email: dyna@revistadyna.com

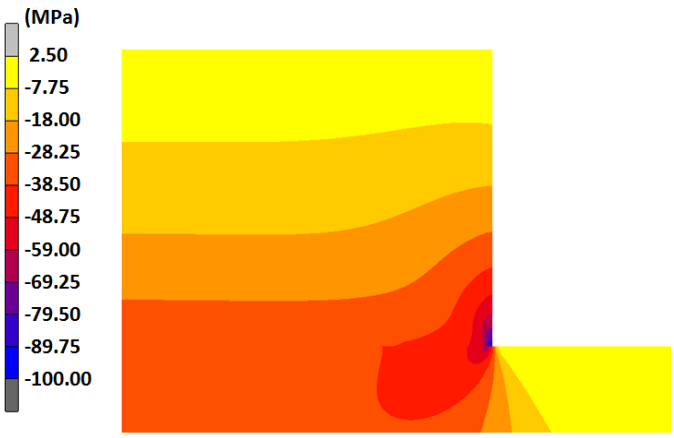

(a)

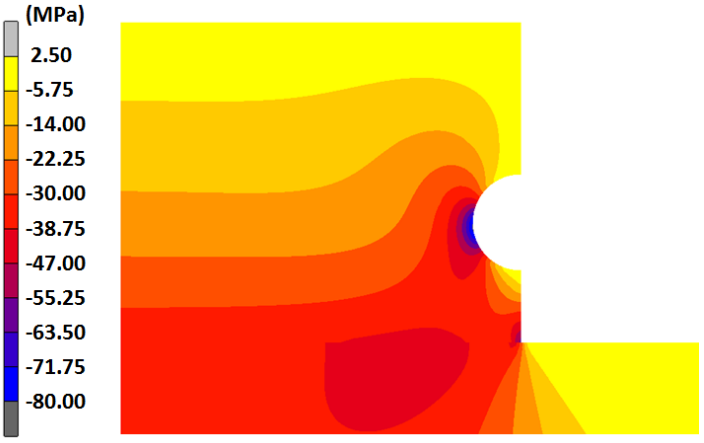

(b)

Fig. 5. Radial stress distribution for (*a*) *unnotched hub, notched hubs:* (*b*) *low notch radius placed close to interference* ($\lambda = 0.4$).

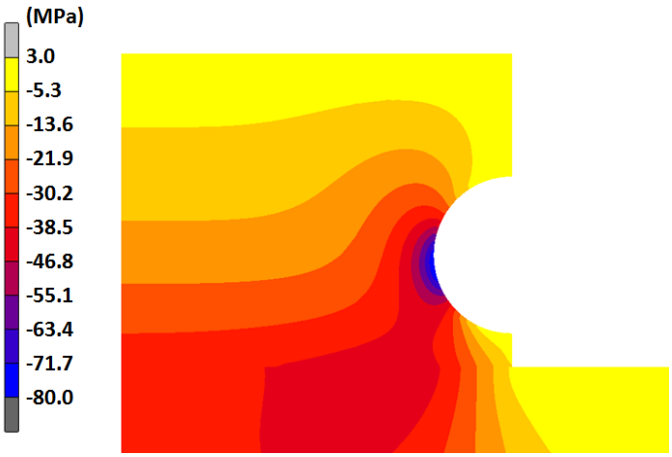

(c)

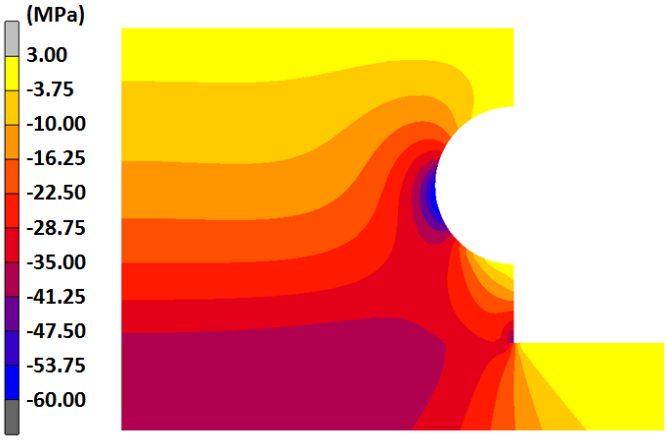

(d)

Fig. 5 (*cont.*). *Radial stress distribution notched hubs:* (*c*) *high notch radius placed close to interference* ($\lambda = 0.6$) *and* (*d*) *high notch radius placed far from interference* ($\lambda = 0.7$).

To achieve a better understanding of the effect of notch radius, a dimensionless parameter is defined as $2r_m/l$. This parameter represents the relative size of the notch in terms of the hub length. Thus, this parameter tends to 0 when a groove radius is pretty lower than the hub length. Besides it tends to 1 in the opposite case, i.e., when the groove radius approaches the hub half-length. The variations of K_j factors as a function of the ratio $2r_m/l$ are shown in Fig. 6.

Publicaciones DYNA SL -- c) Mazarredo nº69 - 4º -- 48009-BILBAO (SPAIN)
Tel +34 944 237 566 – www.revistadyna.com - email: dyna@revistadyna.com

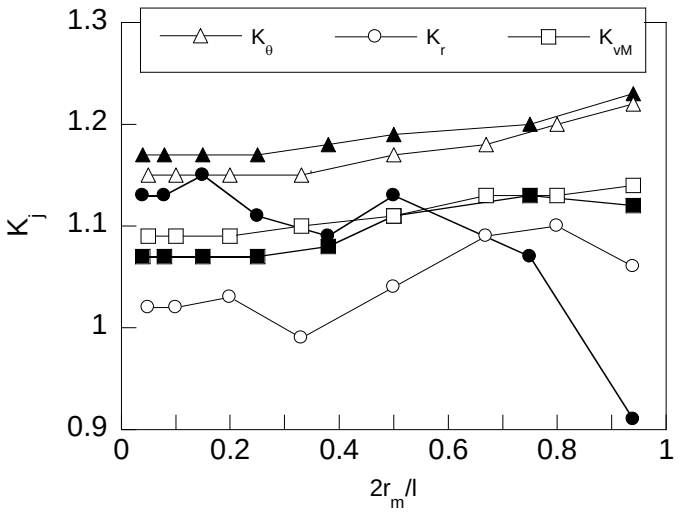

Fig. 6. Stress concentration factors calculated at the interface as a function of ratio $2r_m/l$. Filled symbols corresponding to $(\lambda, \xi)_1$ and open symbols to $(\lambda, \xi)_2$.

Up to values $2r_m/l = 0.2$ (i.e., the hub length l is 5 times the notch diameter, $2r_m$), all the K_j factors are almost constant. High values of $2r_m/l$ are only of academic interest since such values are senseless from the engineering point of view since most of the hub sectional area is removed by the groove as Fig. 7 shows. K_θ and K_{vM} factors are practically not dependent on the parameters (λ, ξ) analysed and, only for $2r_m/l$ higher values, significant variations in K_r are observed.

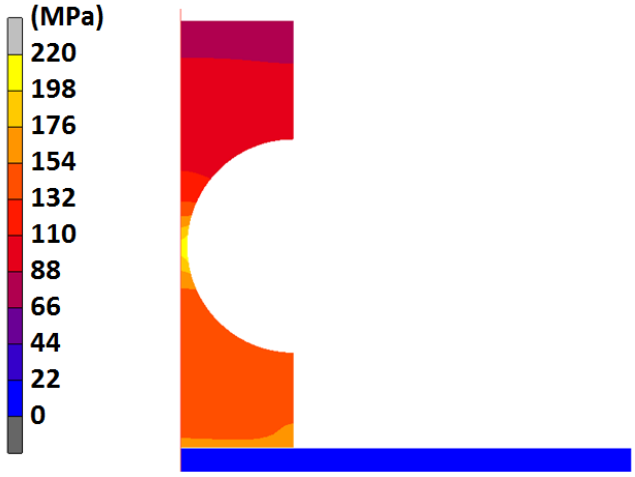

Fig. 7. von Mises stress distribution in a hub with a ratio $2r_m/l=0.94$.

5.- CONCLUSIONS

In this work, we have carried out calculations using the finite element method to evaluate the stress state in interference fits when a circumferential notch is milled on the hub surface.

In order to verify how notch geometry reduces or eliminates the stress concentration in the external cylinder of the fit, theoretical stress concentration factors K_j for radial ($j \equiv r$), hoop ($j \equiv \theta$) and von Mises ($j \equiv vM$) stress were defined.

Publicaciones DYNA SL -- c) Mazarredo nº69 - 4º -- 48009-BILBAO (SPAIN)
Tel +34 944 237 566 – www.revistadyna.com - email: dyna@revistadyna.com

According to numerical simulations, the K_j factors are not dependent on the radial interference, δ. Furthermore, they do not depend on hub length whereas this one will be at least 2 times lower than the shaft length and 10 times higher than the groove radii. We have found that the values of K_θ (K_r) significantly decrease (increase) with the radii ratio R/r_0, while K_{vM} practically remains constant.

We have also considered two different groove geometries characterized by dimensionless parameters (λ, ξ). K_r is the more sensible factor to changes in the notch geometry being almost negligible the variations of the others factors. Thus, when the values of (λ, ξ) are around 0.5, i.e., in the case $(\lambda, \xi)_2$, $K_r \leq 1.10$ for all the cases analysed, thereby the beneficial effect of the groove is probed when the right geometry is used. So, K_r is the design factor more adequate for finding out the groove geometry which reduces in an optimal way the stress concentrations in the hub of a press fit. This question will be discussed in a future investigation.

BIBLIOGRAPHY

[1] Horger OJ, Nelson CW. "Design of Press and Shrink Fitted Assemblies". *Journal of Applied Mechanics*. Vol.4-4 A183-A187.

[2] Peterson RE, Wahl AM. "Fatigue of shafts at fitted members with related photoelastic analysis". *Journal of Applied Mechanics*. Vol.2 p.1-11.

[3] Prasad SN, Dasgupta S. "Axisymmetric shrink fit problems of the elastic cylinder of finite length". *Journal of Elasticity*. Vol.7-3 p.225-242. DOI: http://dx.doi.org/10.1007/BF00041071.

[4] Siva Prasad N, Sashikanth P, Ramamurti V. "Stress distribution in interference joints". *Computers & Structures*. Vol.51-5 p.535-540. DOI: http://dx.doi.org/10.1016/0045-7949(94)90060-4.

[5] Zhang Y, McClain B, Fang XD. "Design of interference fits via finite element method". *International Journal of Mechanical Sciences*. Vol.42 p.1835-1850. DOI: http://dx.doi.org/10.1016/S0020-7403(99)00072-7.

[6] Yang GM, Coquille JC, Fontaine JF et al. "Influence of roughness on characteristics of tight interference fit of a shaft and a hub". *International Journal of Solids and Structures*. Vol.38-42 p.7691-7701. DOI: http://dx.doi.org/10.1016/S0020-7683(01)00035-X.

[7] Özel A, Temiz Ş, Aydin MD et al. "Stress analysis of shrink-fitted joints for various fit forms via finite element method". *Materials & Design*. Vol.26-4 p.281-289. DOI: http://dx.doi.org/10.1016/j.matdes.2004.06.014.

[8] Sen S, Aksakal B. "Stress analysis of interference fitted shaft-hub system under transient heat transfer conditions". *Materials & Design*. Vol.25-5, p.407-417. DOI: http://dx.doi.org/10.1016/j.matdes.2003.11.009.

[9] Parsons B, Wilson EA. "A method for determining the surface contact stresses resulting from interference fits". *Journal of Manufacturing Science and Engineering ASME*. Vol.92-1 p.208-218. DOI: http://dx.doi.org/10.1115/1.3427710.

[10] Szwedowicz D, Bedolla J. "Contact notch stress assessment within frictional contact joints". *DYNA*. Vol.79-171 p.88-96.

[11] Oda J, Sakamoto J, San K. "A method for producing a uniform contact stress distribution in composite bodies with interference". *Structural Optimization*. Vol.3-1 p.23-28. DOI: http://dx.doi.org/10.1007/BF01743486.

[12] Güven U. "Stress distribution in shrink fit with elastic-plastic hub exhibiting variable thickness". *International Journal of Mechanical Sciences*. Vol.35-1 p.39-46. DOI: http://dx.doi.org/10.1016/0020-7403(93)90063-Z.

[13] Pérez-Cerdán JC, Lorenzo M, Blanco C. "Stress Concentrations in Interference Fit Joints with Chamfered Hubs". *Applied Mechanics and Materials*. Vol.184 p.489-492. DOI: http://dx.doi.org/10.4028/www.scientific.net/AMM.184-185.489.

[14] Jones IA, Truman CE, Booker JD, Lambertin M. "Photoelastic investigation of slippage in shrink-fit assemblies". *Experimental Mechanics*, Vol.48 p.621-633. DOI: http://dx.doi.org/10/1007s11340-008-9140-6.

[15] Lewis R., Marshall MB, Dwyer-Joyce RS. "Measurement of interface pressure in interference fits". *Journal of Mechanical Engineering Science Part C*, Vol.219-2 p.127-139. DOI: http://dx.doi.org/10.1243/095440605X8402.

[16] Marshall MB, Lewis R, Dwyer-Joyce RS, Demilly F, Flament Y. "Ultrasonic measurement of railway wheel hub–axle press-fit contact pressures". *Proceedings of the Institution of Mechanical Engineers, Part F: Journal of Rail and Rapid Transit,* Vol.225(3) p.287-298. DOI: http://dx.doi.org/10.1177/2041301710392482.

[17] Conway HD, Farnham KA. "Contact stresses between cylindrical shafts and sleeves". *International Journal of Engineering Sciences*. Vol.5-7 p.541-554. DOI: http://dx.doi.org/10.1016/0020-7225(67)90032-8.

[18] Mather J, Baines BH. "Distribution of stress in axially symmetrical shrink-fit assemblies". *Wear*. Vol.21-2 p.339-360. DOI: http://dx.doi.org/10.1016/0043-1648(72)90008-7.

[19] Grimm TR, Chiu AC. *Design of hubs to minimize interface stresses - a finite element study*. En: *Computers in Engineering: Proc. of the 1988 ASME International Computers in Engineering Conference and Exhibition*, (San Francisco, California, July 31th - Aug. 4th, 1988), 1988, p.85-91.

[20] Truman CE, Booker JD. "Analysis of a shrink-fit failure on a gear hub/shaft assembly". *Engineering Failure Analysis*. Vol.14-4 p.557-572. DOI: http://dx.doi.org/10.1016/j.engfailanal.2006.03.008.

[21] Lanoue F, Vadean A, Sanschagrin B. "Finite element analysis and contact modelling considerations of interference fits for fretting fatigue strength calculations". *Simulation Modelling Practice and Theory*. Vol.17-10, p.1587-1602. DOI: 10.1016/j.simpat.2009.06.017.

[22] Shigley JE, Mischke CR, Brown T. *Standard handbook of machine design*. 1st edition. New York: McGraw-Hill, 1986. 1200p. ISBN: 9780071501439.

[23] Belytschko T, Liu WK, Moran B, Elkhodary K. Nonlinear finite elements for continua and structures. Second edition, Chichester, West Sussex (United Kingdom): John Wiley & Sons, 2013. 816p. ISBN: 978-1-118-63270-3.

Publicaciones DYNA SL -- c) Mazarredo nº69 - 4º -- 48009-BILBAO (SPAIN)
Tel +34 944 237 566 – www.revistadyna.com - email: dyna@revistadyna.com

[24] Croccolo D, Vincenzi N. "Stress concentration factors in compression-fit couplings". *Proceedings of the Institution of Mechanical Engineers, Part C: Journal of Mechanical Engineering Science*. Vol.224-6 p.1143-1152. DOI: http://dx.doi.org/10.1243/09544062JMES1881.

[25] Bijak-Żochowski M, Marek P, Tracz M. "On methods of reduction and elimination of stress singularities in some elastic contact problems". *International Journal of Mechanical Science.* Vol.36-4 p.279-296. DOI: http://dx.doi.org/10.1016/0020-7403(94)90035-3.

[26] Castagnetti D, Dragoni E. "Optimal aspect ratio of interference fits for maximum load transfer capacity". *The Journal of Strain Analysis for Engineering Design*. Vol.40-2 p.177-184. DOI: http://dx.doi.org/10.1243/030932405X7737.

AKNOWLEGMENTS

The authors wish to acknowledge the financial support provided by the Spanish Institution "Memoria D. Samuel Solórzano Barruso" (USAL, Grant FS/21-2012 and Grant 463AC06).